

Dissociative phosphine exchange for cyclopentadienylmolybdenum(III) systems. Bridging the gap between Werner-like coordination chemistry and low-valent organometallic chemistry [☆]

Audrey A. Cole, James C. Fettinger, D. Webster Keogh, Rinaldo Poli ^{*}

Department of Chemistry and Biochemistry, University of Maryland, College Park, MD 20742, USA

Received 1 February 1995; revised 22 May 1995

Abstract

Several phosphine exchange processes on 17-electron $\text{CpMoCl}_2(\text{PR}_3)_2$ systems have been investigated. The exchange of two PPh_3 ligands with either two PMe_3 ligands or with $\text{Ph}_2\text{PCH}_2\text{CH}_2\text{PPh}_2$ (dppe) is complete within a few minutes at -80°C . Equally fast is the exchange of two PEt_3 ligands with two PMe_3 ligands. On the other hand, the exchange of two PEt_3 ligands with dppe is much slower ($t_{1/2} \approx 15$ min to a few hours at r.t.), with excess dppe accelerating the exchange and free PEt_3 retarding it. The self-exchange reaction of PMe_3 is extremely slow (less than 25% exchange at r.t. in 6 h at r.t.) and an analysis of the initial rate of this reaction shows a two-term rate law with one $[\text{PMe}_3]$ -dependent and one independent term. Finally, PMe_3 self-exchange on $\text{Cp}^*\text{MoCl}_2(\text{PMe}_3)_2$ proceeds over one order of magnitude faster than for the corresponding Cp system, with a substantially $[\text{PMe}_3]$ -independent rate law. All these data are indicative of a dominant dissociative exchange mechanism involving rupture of the Mo-PR_3 bond in the slow step and formation of a 15-electron intermediate. The rate of phosphine dissociation qualitatively correlates with the Mo-P distance in the 17-electron starting complex. Only for the $\text{Cp-MoCl}_2(\text{PMe}_3)_2$ system is phosphine dissociation sufficiently slowed down so that the alternative associative exchange pathway becomes competitive. Possible reasons for a low activation barrier in these dissociative exchanges are discussed.

Keywords: Kinetics and mechanism; Dissociative phosphine substitution; Molybdenum complexes; Cyclopentadienyl complexes

1. Introduction

Ligand substitution on organometallic compounds is a topic of long-standing interest [1–4], since an elementary step involving a ligand dissociation, association or substitution is always involved in any catalytic cycle involving transition metal organometallics. After much emphasis was initially given to Tolman's 16/18-electron rule [5], the mechanism of substitution in 17-electron compounds has been shown to play an important role and has recently been the subject of detailed studies [6]. In brief, it has been shown that organometallic radicals (typically low-oxidation state, π -acid stabilized molecules, therefore with a low-energy SOMO and a high tendency to reach a saturated configuration by dimerization or by reduction) undergo very rapid *associative* substitution processes, as opposed to their saturated analogs for which much more sluggish substitutions typically follow a dissociative path. Perhaps the most ground-breaking

studies have been those of Poë and co-workers [7] and Herington and Brown [8], demonstrating associative substitution for the transient $\text{M}(\text{CO})_5$ ($\text{M} = \text{Mn}, \text{Re}$) radicals, and of Basolo and co-workers [9], showing that associative substitution for $\text{V}(\text{CO})_6$ proceeds 10^{10} times faster than for the corresponding $\text{Cr}(\text{CO})_6$. The difference has been attributed to the absence of an electronic barrier to ligand association for the 17-electron complex [10], although a greater steric barrier is present with respect to the dissociative path.

Dissociative ligand substitution is thought to be unfavourable for 17-electron organometallic compounds because it requires the involvement of highly unsaturated (15-electron) intermediates. Indeed, only *very slow* first-order processes have been observed for 17-electron systems where the steric bulk of the ligands strongly disfavors an otherwise faster associative path [11].

In this contribution we shall show a *fast* and *dissociative* phosphine exchange process for the 17-electron half-sandwich $\text{Mo}(\text{III})$ system $\text{CpMoCl}_2\text{L}_2$ and for a Cp^* analog, and discuss the possible reasons for this behavior.

^{*} Dedicated to Professor Fred Basolo on the occasion of his 75th birthday.

^{*} Corresponding author.

2. Experimental

2.1. General

All operations were carried out under an atmosphere of dinitrogen using standard glove-box and Schlenk-line techniques. Solvents were dehydrated by standard methods, deoxygenated, and distilled directly from the dehydrating agent under dinitrogen prior to use. Samples for EPR spectra were placed in 3 mm glass tubes and measured on a Bruker ER200 spectrometer, using DPPH ($g = 2.004$) as a calibrant. Samples for ^1H and ^{31}P NMR in thin-walled 5 mm glass tubes were measured on a Bruker WP200 spectrometer. The ^1H NMR spectra were calibrated against the residual proton signal of the deuterated solvents. The ^{31}P NMR were calibrated against 85% H_3PO_4 in a capillary tube which was placed in a different 5 mm glass tube, containing the same deuterated solvent used for the measurement. For the purpose of quantitative determination of the relative phosphine concentrations, the ^{31}P NMR spectra were collected with a 10 s relaxation delay between pulses.

Complexes $\text{CpMoCl}_2(\text{PMe}_3)_2$ [12], $\text{CpMoCl}_2(\text{dppe})$ [13], $\text{CpMoCl}_2(\text{PPh}_3)_2$ [14] and $\text{Cp}^*\text{MoCl}_2(\text{PMe}_3)_2$ [15] were prepared as previously described. The phosphine ligands dppe (Strem), PEt_3 (Strem), PMe_3 (Aldrich), and $\text{P}(\text{CD}_3)_3$ (Aldrich) were used as received.

2.2. EPR study of $\text{CpMoCl}_2(\text{PEt}_3)_2/\text{dppe}$ exchange

(a) Constant $\text{dppe}/\text{CpMoCl}_2(\text{PEt}_3)_2$ ratio, variable $\text{PEt}_3/\text{CpMoCl}_2(\text{PEt}_3)_2$ ratio

$\text{CpMoCl}_2(\text{PPh}_3)_2$ (0.127 g, 0.167 mmol) was dissolved in CH_2Cl_2 (48 ml). Aliquots (5 ml, 0.017 mmol) of this solution were treated with varying amounts of PEt_3 (5.2, 12.8, 17.7, 19.2, 25.1 μl) to prepare five solutions of $\text{CpMoCl}_2(\text{PEt}_3)_2$ with various excesses of PEt_3 (0, 3, 5, 5.6 and 8 mol/mol, respectively). The formation of $\text{CpMoCl}_2(\text{PEt}_3)_2$ is rapid and quantitative [14] and is indicated by a color change from dark green to brown-green. To each of these solutions was added dppe (0.135 g, 0.34 mmol, or 20 mol/mol). Aliquots of each solution were then transferred into EPR tubes, which were flamed sealed and kept at 27 °C. The exchange was qualitatively followed by monitoring the EPR signal.

(b) Variable $\text{dppe}/\text{CpMoCl}_2(\text{PEt}_3)_2$ ratio, constant $\text{PEt}_3/\text{CpMoCl}_2(\text{PEt}_3)_2$ ratio

A 3.5 mM solution of $\text{CpMoCl}_2(\text{PPh}_3)_2$ was prepared by dissolving 152 mg of the complex (0.20 mmol) in 57 ml of CH_2Cl_2 in a Schlenk flask. To this solution was added PEt_3 (148 μl , 1.00 mmol) by a syringe to convert the complex quantitatively to $\text{CpMoCl}_2(\text{PEt}_3)_2$ and to leave an excess amount (3 mol/mol) of PEt_3 . Three Schlenk flasks were charged with 60 mg (0.15 mmol), 84 mg (0.21 mmol) and 104 mg (0.26 mmol), respectively, of dppe. To each of these Schlenk flasks was added 3.0 ml of the $\text{CpMoCl}_2(\text{PEt}_3)_2$

solution (1.5×10^{-2} mmol), and an aliquot of each of the resulting solutions was rapidly transferred into an EPR tube and monitored by EPR at 27 °C.

2.3. ^{31}P NMR studies of $\text{CpMoCl}_2(\text{PR}_3)_2/\text{PR}'_3$ exchange processes

(a) Exchange reaction of $\text{CpMoCl}_2(\text{PPh}_3)_2$ with PMe_3

In a Schlenk flask $\text{CpMoCl}_2(\text{PPh}_3)_2$ (34.4 mg, 0.0455 mmol) was dissolved in CD_2Cl_2 (1 ml). After cooling the flask to -80 °C, PMe_3 (0.047 μl , 0.45 mmol) was added via a syringe. By carrying out all operations at -80 °C, the solution was then transferred into a 5 mm NMR tube, which was flame sealed and immediately inserted into the NMR probe, which had been pre-cooled to -80 °C. The reaction was monitored by observing the ^{31}P NMR resonances of the free phosphines. The first spectrum, taken 8 min after mixing, shows $[\text{PPh}_3]/[\text{PMe}_3] = 1:3.73$, and this ratio remains relatively unchanged after 19 min. By using the average ratio measured between 8 and 19 min as a measure of the final concentration ratio ($1:3.86 \pm 0.14$), it is estimated that the reaction is more than 86% complete after 8 min at -80 °C.

(b) Exchange reaction of $\text{CpMoCl}_2(\text{PPh}_3)_2$ with dppe

$\text{CpMoCl}_2(\text{PPh}_3)_2$ (0.0125 g, 0.0165 mmol) was dissolved in CD_2Cl_2 (1 ml). After cooling to -80 °C, dppe (0.0658 g, 0.165 mmol) was added and the solution was used to prepare a sample for ^{31}P NMR monitoring as described in the previous section. The first spectrum, taken 3 min after mixing, shows a $[\text{PPh}_3]/[\text{dppe}]$ ratio of 1:3.54 and this ratio remains approximately constant over 39 min. By using the average ratio measured between 3 and 39 min as a measure of the final concentration ratio ($1:3.40 \pm 0.11$), it is estimated that the reaction is more than 89% complete after 3 min at -80 °C.

(c) Exchange reaction of $\text{CpMoCl}_2(\text{PEt}_3)_2$ with PMe_3

$\text{CpMoCl}_2(\text{PEt}_3)_2$ was generated in situ by reacting $\text{CpMoCl}_2(\text{PPh}_3)_2$ (0.0356 g, 0.0471 mmol) with PEt_3 (0.014 ml, 0.094 mmol) in CD_2Cl_2 (1 ml). An immediate color change from dark green to green-brown indicated the quantitative transformation to $\text{CpMoCl}_2(\text{PEt}_3)_2$. By carrying out all subsequent operations as described in Part (a), PMe_3 (0.049 ml, 0.47 mmol) was added and the sample was transferred into the NMR tube for monitoring by ^{31}P NMR. The first spectrum was taken 11 min after mixing and shows a $[\text{PPh}_3]:[\text{PEt}_3]:[\text{PMe}_3]$ ratio of 1:1.09:4.56. This ratio remains approximately constant over 25 min. By using the average ratio measured between 11 and 25 min as a measure of the final concentration ratio ($1:1.05 \pm 0.04:4.62 \pm 0.05$), it is estimated that the reaction is more than 94% complete after 11 min at -80 °C.

A second experiment for this exchange reaction was carried out in the presence of an excess amount of free PEt_3 . $\text{CpMoCl}_2(\text{PEt}_3)_2$ was synthesized in situ by addition of 32 μl of PEt_3 (2.2×10^{-1} mmol) to a solution of 16.5 mg of

Table 1
Observed rate constants (from initial rates) measured for reactions (6) and (8)

Ring	[(Ring)MoCl ₂ (PMe ₃) ₂] (M)	[PMe ₃ -d ⁹] (M)	k _{obs} × 10 ⁵ (s ⁻¹)
Cp	0.0448	0.600	0.60 ± 0.02
Cp	0.0399	1.586	1.19 ± 0.05
Cp	0.0360	1.807	1.51 ± 0.06
Cp*	0.0489	0.489	26.9 ± 1.0
Cp*	0.0441	1.323	30.1 ± 2.3
Cp*	0.0406	2.030	32.3 ± 1.1

CpMoCl₂(PPh₃)₂ (2.18 × 10⁻² mmol) in 1 ml of CD₂Cl₂. After cooling to -80 °C, PMe₃ (22 μl, 2.2 × 10⁻¹ mmol) was added and the solution was monitored by ³¹P NMR under the same conditions described in the previous sections. From 2 to 39 min, the approximate ratio of the integrated intensities does not significantly change, indicating that the exchange is, once again, practically complete by the time the first spectrum is measured.

2.4. ¹H NMR study of the CpMoCl₂(PMe₃)₂/PMe₃-d⁹ exchange

CpMoCl₂(PMe₃)₂ (0.0723 g, 0.191 mmol) was dissolved in C₆D₆ (4 ml). Three aliquots (0.500 ml, 0.0239 mmol) were transferred into NMR tubes and cooled to 77 K. PMe₃-d⁹ was then added to each of the three tubes by a syringe (33 μl, 0.32 mmol; 99 μl, 0.95 mmol; and 164 μl, 1.20 mmol; respectively, giving [PMe₃-d⁹]/[CpMoCl₂(PMe₃)₂] ratios of 13.4, 39.7 and 50.2). The tubes were then flame sealed and the reactions were monitored by observing the growth of the free PMe₃ resonances in the ¹H NMR at 27 °C. The concentration of the free PMe₃ was determined by integration versus the residual proton peak of the deuterated solvent, which was calibrated against three standard solutions of PMe₃ in C₆D₆ of known concentrations. Such measurements provided the concentration of the residual protonated isotopomer in the solvent as [C₆D₅H] = (1.426 ± 0.047) × 10⁻¹ M. Only the data collected in the first 450 min, corresponding to less than 25% exchange, were used to calculate the initial rates of the reactions (see Table 1).

After the tubes were allowed to rest at room temperature for several days, an orange crystalline solid began precipitating. This solid was isolated and investigated spectroscopically. The EPR spectrum of a CH₂Cl₂ solution, when recorded immediately, showed a doublet of triplets (g = 2.000, a_{P(t)} = 20 G, a_{P(d)} = 26 G). After this solution was allowed to remain overnight at room temperature, however, the EPR spectrum had changed and showed a binomial triplet (g = 1.981, a_p = 16 G) indicative of the starting material, CpMoCl₂(PMe₃)₂.

2.5. ¹H NMR study of the Cp*MoCl₂(PMe₃)₂/PMe₃-d⁹ exchange

In a similar fashion to the previous reaction series, Cp*MoCl₂(PMe₃)₂ (0.047 g, 0.103 mmol) was dissolved in C₆D₆ (2 ml), and three aliquots (400 μl, 0.0206 mmol) were transferred into NMR tubes and the solutions frozen at 77 K. PMe₃-d⁹ was added to each of the tubes (21 μl, 0.206 mmol; 64 μl, 0.617 mmol; and 107 μl, 1.03 mmol; respectively, corresponding to [PMe₃-d⁹]/[Cp*MoCl₂(PMe₃)₂] ratios of 10.0, 30.0 and 50.0). The tubes were then sealed and the reactions monitored as previously discussed. The data collected in the first 20 min, corresponding to less than 25% exchange, were used to calculate the initial rates of the reactions (see Table 1).

2.6. Cyclic voltammetry (CV) study of CpMoCl₂(PEt₃)₂ in the presence of dppe

Cyclic voltammograms were recorded with an EG&G 362 potentiostat connected to a Macintosh computer through MacLab hardware/software. The electrochemical cell used consisted of a modified Schlenk tube with a Pt counter electrode sealed through uranium glass/Pyrex glass seals. The cell was fitted with a Ag/AgCl reference electrode and a Pt disk working electrode. All half-wave potentials were measured and are reported with respect to the ferrocene/ferrocenium (fc/fc⁺) couple. The ferrocene was added to the solution at the beginning of each measurement as an internal standard, and the potentials are not IR corrected. CpMoCl₂(PEt₃)₂ was generated in situ from CpMoCl₂(PPh₃)₂ (0.0486 g, 0.0642 mmol) and PEt₃ (0.019 ml, 0.13 mmol) in CH₂Cl₂ (5 ml). The electrochemical cell was charged with dppe (0.054 g, 0.135 mmol), n-Bu₄N⁺PF₆⁻ (155 mg, 0.4 mmol), CH₂Cl₂ (3.0 ml), and an aliquot of the CpMoCl₂(PEt₃)₂ solution (1.0 ml, 0.013 mmol).

2.7. ¹H NMR study of the [CpMoCl₂(PEt₃)₂]⁺/dppe exchange

{CpMoCl₂}_n (0.237 g, 1.02 mmol of Mo) was suspended in THF (15 ml), followed by the addition of PEt₃ (0.305 ml, 2.06 mmol). The solution was stirred at room temperature for 3 h, resulting in the formation of a brown solution of CpMoCl₂(PEt₃)₂ as previously described [14]. To a 1.2 ml portion of this solution (0.082 mmol of CpMoCl₂(PEt₃)₂) was added AgPF₆ (30 mg, 0.11 mmol). The complete consumption of the Mo(III) material was verified by the disappearance of the EPR signal. The solution was evaporated to dryness, the residue was extracted with 1 ml of acetone-d⁶, and the resulting solution was filtered. The main portion of this solution was utilized for a variable temperature ¹H NMR characterization (see Results). A 0.15 ml portion of this solution (0.012 mmol of [CpMoCl₂(PEt₃)₂]⁺) was introduced into an NMR tube that had been charged with dppe (48 mg, 0.12 mmol) and acetone-d⁶ (0.70 ml). ¹H and ³¹P

Table 2
Crystal data for both polymorphs of $\text{CpMoCl}_2(\text{PEt}_3)_2$

	A	B
Empirical formula	$\text{C}_{17}\text{H}_{35}\text{Cl}_2\text{MoP}_2$	$\text{C}_{17}\text{H}_{35}\text{Cl}_2\text{MoP}_2$
Formula weight	468.23	468.23
Temperature (K)	153(2)	153(2)
Wavelength (Å)	0.71073	0.71073
Crystal system	monoclinic	orthorhombic
Space group	$P2_1/n$	$P2_12_12_1$
<i>a</i> (Å)	8.1158(9)	11.2351(6)
<i>b</i> (Å)	13.277(2)	12.3171(5)
<i>c</i> (Å)	19.248(2)	15.3937(7)
β (°)	90.063(10)	90
<i>V</i> (Å ³)	2074.0(4)	2130.2(2)
<i>Z</i>	4	4
d_{calc} (Mg m ⁻³)	1.500	1.460
μ (Mo K α) (mm ⁻¹)	1.040	1.013
Reflections collected	3752	4092
Independent reflections	3642 ($R_{\text{int}} = 0.0777$)	3748 ($R_{\text{int}} = 0.0186$)
Data/restraints/parameters	3642/0/184	3748/0/206
$T_{\text{max}}/T_{\text{min}}$	1.164	1.182
Goodness-of-fit on F^2	1.098	1.034
R^a	0.0430	0.0184
R_w^b	0.1160	0.0440

$$^a R = \sum \|F_o\| - \|F_c\| / \sum \|F_o\|$$

$$^b R_w = [\sum w(|F_o| - |F_c|)^2 / \sum w|F_o|^2]^{1/2}; w = 1/\sigma^2(|F_o|)$$

Table 3
Atomic coordinates ($\times 10^4$) and equivalent isotropic displacement parameters ($\text{Å}^2 \times 10^3$) for $\text{CpMoCl}_2(\text{PEt}_3)_2$ (polymorph A)

	<i>x</i>	<i>y</i>	<i>z</i>	U_{eq}^a
Mo(1)	2261(1)	1418(1)	3659(1)	15(1)
P(1)	669(1)	1287(1)	2529(1)	17(1)
P(2)	2698(1)	2556(1)	4698(1)	19(1)
Cl(1)	-565(1)	1409(1)	4138(1)	24(1)
Cl(2)	3343(1)	2936(1)	3063(1)	27(1)
C(1)	4149(2)	370(1)	3197(1)	24(1)
C(2)	4782(2)	757(1)	3836(1)	20(1)
C(3)	3766(2)	392(1)	4383(1)	21(1)
C(4)	2505(2)	-219(1)	4083(1)	25(1)
C(5)	2742(2)	-233(1)	3350(1)	20(1)
C(1A)	4269(2)	601(1)	3254(1)	27(5)
C(2A)	4610(2)	1001(1)	3936(1)	46(5)
C(3A)	3418(2)	201(1)	4327(1)	16(4)
C(4A)	2679(2)	-399(1)	3944(1)	6(3)
C(5A)	3206(2)	-199(1)	3283(1)	25(5)
C(11)	1844(2)	940(1)	1752(1)	25(1)
C(12)	3111(2)	1707(1)	1505(1)	37(1)
C(21)	-377(2)	2445(1)	2252(1)	26(1)
C(22)	-1908(6)	2722(4)	2658(2)	38(1)
C(31)	-979(5)	339(3)	2504(2)	24(1)
C(32)	-2090(6)	345(3)	1860(2)	35(1)
C(41)	1496(5)	2308(3)	5488(2)	27(1)
C(42)	1788(6)	1305(3)	5848(2)	38(1)
C(51)	4792(5)	2649(3)	5056(2)	30(1)
C(52)	6023(5)	3221(4)	4608(3)	41(1)
C(61)	2210(5)	3893(3)	4562(2)	28(1)
C(62)	497(5)	4088(3)	4286(3)	40(1)

^a U_{eq} is defined as one third of the trace of the orthogonalized U_{ij} tensor.

NMR monitoring of this solution indicated no change in the appearance of free PEt_3 within 6 h at room temperature.

2.8. X-ray crystallography of $\text{CpMoCl}_2(\text{PEt}_3)_2$

(a) Polymorph A

Single crystals were obtained by extracting the crude product, produced by the $\{\text{CpMoCl}_2\}_n/\text{PEt}_3$ reaction (see previous section), into hot heptane, filtering, and cooling to 0 °C. A dark reddish-black crystal with dimensions $0.49 \times 0.32 \times 0.20$ mm was placed and optically centered on an Enraf-Nonius CAD-4 diffractometer. The cell parameters and crystal orientation matrix were determined from 25 reflections in the range $23.1 < 2\theta < 27.0$ and further confirmed with axial photographs. Data were collected (Mo K α) with $\omega/2\theta$ scans over the range $2.3 < \theta < 25.0$. Periodical monitoring of three nearly orthogonal standard reflections showed no significant variation of intensity. The data were corrected for Lorentz and polarization factors, and for absorption on the basis of six ψ scan reflections. The systematic absences from the data uniquely determined the space group as monoclinic $P2_1/n$. The structure was solved by direct methods, which located the Mo, Cl and P atoms. The remaining non-hydrogen atoms were found from two subsequent difference-Fourier maps. Hydrogen atoms were placed in calculated positions: $d(\text{C-H}) = 0.950$ with $U = 1.2U$ -(parent) for aromatic hydrogen, $d(\text{C-H}) = 0.980$ with $U = 1.5U$ (parent) for methyl hydrogens, and $d(\text{C-H}) = 0.990$ and $U = 1.2U$ (parent) for methylene hydrogens. Continued refinement and an additional difference-Fourier map revealed a second orientation of the cyclopentadienyl ring; the final occupancy ratio of the major:minor component was 0.77:0.23. The two individual rings were then refined with the hydrogen atoms placed, as before, in calculated positions. Crystal data are assembled in Table 2, atomic coordinates are listed in Table 3, and selected bond distances and angles are given in Table 4.

Table 4
Selected bond lengths (Å) and angles (°) for $\text{CpMoCl}_2(\text{PEt}_3)_2$

Polymorph	A	B
Mo(1)-Cl(1)	2.4735(10)	2.4754(6)
Mo(1)-Cl(2)	2.4787(10)	2.4776(6)
Mo(1)-P(1)	2.5332(10)	2.5239(6)
Mo(1)-P(2)	2.5306(10)	2.5239(6)
Mo(1)-CNT	1.940(2)	1.951(2)
Cl(1)-Mo(1)-Cl(2)	120.38(3)	120.53(2)
Cl(1)-Mo(1)-P(1)	81.24(3)	80.35(2)
Cl(1)-Mo(1)-P(2)	80.62(3)	79.27(2)
Cl(1)-Mo(1)-CNT	118.0(1)	121.6(1)
Cl(2)-Mo(1)-P(1)	80.79(3)	78.91(2)
Cl(2)-Mo(1)-P(2)	80.25(3)	82.64(2)
Cl(2)-Mo(1)-CNT	121.6(1)	117.9(1)
P(1)-Mo(1)-P(2)	142.16(3)	140.24(2)
P(1)-Mo(1)-CNT	108.7(1)	109.8(1)
P(2)-Mo(1)-CNT	109.1(1)	109.9(1)

Table 5
Atomic coordinates ($\times 10^4$) and equivalent isotropic displacement parameters ($\text{\AA}^2 \times 10^3$) for $\text{CpMoCl}_2(\text{PEt}_3)_2$ (polymorph B)

	x	y	z	U_{eq}^a
Mo(1)	2289(1)	566(1)	9129(1)	15(1)
Cl(1)	4224(1)	1526(1)	9110(1)	28(1)
Cl(2)	1428(1)	-171(1)	7769(1)	27(1)
P(1)	3657(1)	-1020(1)	8844(1)	18(1)
P(2)	1686(1)	2356(1)	8462(1)	19(1)
C(1)	529(2)	504(2)	9782(2)	26(1)
C(2)	1194(2)	1275(2)	10263(2)	27(1)
C(3)	2153(2)	745(2)	10659(2)	29(1)
C(4)	2097(2)	-355(2)	10440(2)	28(1)
C(5)	1097(2)	-521(2)	9892(2)	27(1)
C(11)	4166(2)	-1172(2)	7717(2)	24(1)
C(12)	4753(2)	-170(2)	7334(2)	30(1)
C(21)	2931(2)	-2332(2)	9039(2)	26(1)
C(22)	3577(3)	-3348(2)	8735(2)	40(1)
C(31)	5092(2)	-1109(2)	9417(2)	25(1)
C(32)	5061(3)	-1048(2)	10404(2)	35(1)
C(41)	2100(2)	2432(2)	7309(2)	28(1)
C(42)	1796(3)	3489(2)	6826(2)	39(1)
C(51)	100(2)	2715(2)	8477(2)	25(1)
C(52)	-706(2)	1981(2)	7928(2)	31(1)
C(61)	2376(3)	3607(2)	8878(2)	28(1)
C(62)	2308(3)	3795(2)	9857(2)	31(1)

^a U_{eq} is defined as one third of the trace of the orthogonalized U_{ij} tensor.

(b) Polymorph B

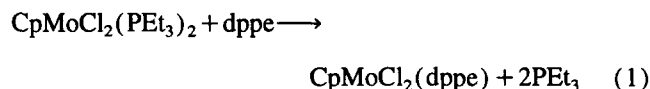
Single crystals were obtained in an identical fashion as described above for polymorph A, except that the filtered heptane solution was cooled to -20°C . A dark reddish-black crystal with dimensions $0.38 \times 0.25 \times 0.18$ mm was placed and optically centered on an Enraf–Nonius CAD-4 diffractometer. All operations were conducted as described above for polymorph A. The systematic absences uniquely determined the space group as orthorhombic $P2_12_12_1$. The structure solution and refinement was as for polymorph A, except that the cyclopentadienyl ring was found to exist in a single orientation. Crystal data are assembled in Table 2, atomic coordinates are listed in Table 5, and selected bond distances and angles are given in Table 4 together with those of polymorph A.

3. Results

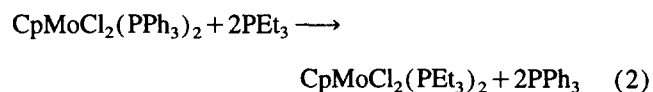
3.1. Reaction rate studies

We have previously reported [16] that the 17-electron organometallic Mo(III) system, $\text{CpMoX}_2(\text{PMe}_3)_2$, exchanges the halide ligands quite slowly by an associative mechanism (either through a 19-electron intermediate or through a 17-electron, ring-slipped intermediate) and have since wondered whether the same mechanism would be effective for the exchange of the phosphine ligands. The halide (I/Cl) exchange was conveniently monitored by EPR spectroscopy since the different species involved in the reac-

tion absorb the radio frequency at sufficiently different field strengths. Use of the EPR technique for the phosphine exchange is much more problematic because (a) complexes with the same halides and different phosphine ligands show EPR spectra with very similar g values [14]; (b) the exchange reactions tend to be, from preliminary experiments, much faster than the halide exchange [14]; and (c) in view of point (a), the formation of intermediate mixed-phosphine complexes would render it very difficult to extract concentration information for all the individual species from EPR data. These problems were partly alleviated by choosing to monitor the $\text{CpMoCl}_2(\text{PEt}_3)_2/\text{dppe}$ exchange:



since (a) the signals are sufficiently separated in the EPR spectrum to allow at least a qualitative analysis of the reaction progress (see Fig. 1); (b) the reaction is relatively slow (half-lives are of the order of 15 min to a few hours at room temperature); (c) the chelating nature of the incoming phosphine suppresses the accumulation of a mixed phosphine intermediate. This reaction is known to proceed to completion [14] when a large excess of dppe is used. A complication arises from the reported tendency of the required starting material, $\text{CpMoCl}_2(\text{PEt}_3)_2$, when isolated as a solid, to lose phosphine [14]. To circumvent this problem, the compound was generated in situ by phosphine exchange according to



It was previously shown by EPR that this reaction is rapid and quantitative. Furthermore, the starting PPh_3 complex is easily prepared and readily crystallizes in an analytically pure form [14].

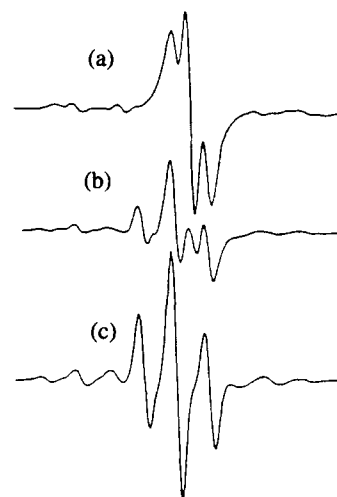


Fig. 1. EPR spectra for a representative $\text{CpMoCl}_2(\text{PEt}_3)_2/\text{dppe}$ exchange run: (a) before adding dppe; (b) $t = 23$ min; (c) $t = \infty$ (spectrum of $\text{CpMoCl}_2(\text{dppe})$). Solvent CH_2Cl_2 ; $T = 27^\circ\text{C}$.

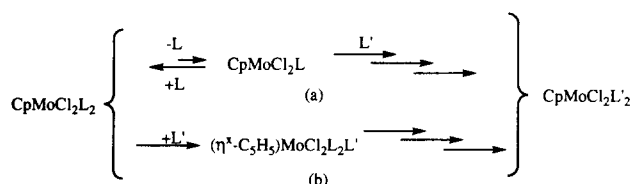
Table 6
Values of the first-order (dissociative) rate constants for phosphine exchange reactions

Reaction	T (°C)	k ₁ (s ⁻¹)	ΔG* (kJ mol ⁻¹)
CpMoCl ₂ (PPh ₃) ₂ /PMe ₃	-80	> 8.20 × 10 ⁻³	< 54.2
CpMoCl ₂ (PPh ₃) ₂ /dppe	-80	> 1.23 × 10 ⁻²	< 53.6
CpMoCl ₂ (PEt ₃) ₂ /PMe ₃	-80	> 1.56 × 10 ⁻²	< 53.2
CpMoCl ₂ (PMe ₃) ₂ /PMe ₃ -d ⁹	27	(1.65 ± 0.78) × 10 ⁻⁶	106.9 ± 1.2 ^a
Cp*MoCl ₂ (PMe ₃) ₂ /PMe ₃ -d ⁹	27	(2.52 ± 0.09) × 10 ⁻⁴	94.3 ± 0.1 ^b

^a For this exchange, a second-order rate constant (see Eq. (7) and Fig. 3) was also calculated as k₂ = (7.01 ± 0.54) × 10⁻⁶ M⁻¹ s⁻¹.

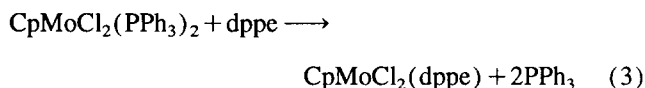
^b For this exchange, a second-order rate constant (see Eq. (7) and Fig. 3) was also calculated as k₂ = (3.53 ± 0.46) × 10⁻⁵ M⁻¹ s⁻¹.

Experiments were performed at various [dppe]/[CpMoCl₂(PEt₃)₂] ratios by keeping the initial concentrations of the Mo complex and excess PEt₃ constant, and also at constant [dppe]/[CpMoCl₂(PEt₃)₂] ratio with variable amounts of excess PEt₃. Due to the extensive signal overlap, the extraction of concentration information from the EPR data was not as accurate as achieved previously for the halide exchange process [16]; therefore accurate kinetic information could not be obtained from this study. Qualitatively, however, we observed a definite acceleration of the reaction by excess dppe and a significant retardation by excess PEt₃. These results are in agreement with a dissociative mechanism and phosphine competition for binding the intermediate (Scheme 1, path (a)), whereas the observed retardation effect by free PEt₃ excludes the alternative associative path (b).

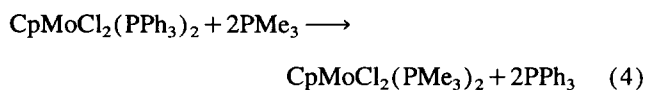


Scheme 1.

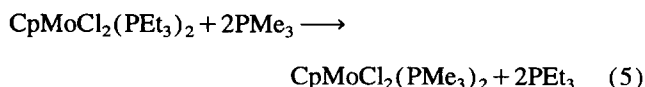
We then turned our attention to other CpMoCl₂(PR₃)₂/PR'₃ exchange processes where PR₃ and PR'₃ were judiciously varied. Previous studies have shown that the relative order of thermodynamic stability for the CpMoCl₂L₂ complexes is: PPh₃ < PMePh₂ ≪ PEt₃ < dppe ≈ PMePh₂ ≪ PMe₃ [14]. We selected the quantitative exchanges of CpMoCl₂(PPh₃)₂ with dppe:



and PMe₃:



and the exchange of CpMoCl₂(PEt₃)₂ with PMe₃:



These reactions could not be monitored by EPR for the reasons discussed above, nor could ¹H NMR be of much value, because the signals due to the 17-electron complexes are broadened beyond detection. The only NMR signals that can be observed are those of the entering and leaving free ligands. These signals are much more distinct in the ³¹P NMR spectrum; therefore ³¹P NMR was the technique of choice for reaction monitoring. All three reactions were found to be practically complete within a few minutes at -80 °C (see Experimental), giving the lower limits for the first-order rate constants reported in Table 6.

These values were calculated by assuming a dissociative mechanism and a first-order integrated rate law, from the estimates of the degree of conversion at the time the first spectrum was measured, as described in Section 2. The assumption of a dissociative pathway, at this point, is strongly suggested by the tremendous rate acceleration for the exchange of CpMoCl₂(PR₃)₂ with dppe on going from the PEt₃ to the PPh₃ complex. On steric grounds, PEt₃ is a smaller ligand (cone angle θ = 132°) than PPh₃ (θ = 145°) [17]; therefore an associative reaction would be expected to be slower for the PPh₃ complex, contrary to the observation. One might argue that the observed pattern of reactivity could be reconciled with an associative path on electronic grounds (PPh₃ is a poorer donor than PEt₃, rendering the PPh₃ starting complex more susceptible to nucleophilic attack by dppe). However, other arguments based on further studies that are discussed below definitely rule out an associative mechanism for this reaction. It should also be pointed out that the Mo–P bond in the bis-PPh₃ complex is quite long (2.546(3) Å) [16], compared to bonds to smaller phosphines in the same class of compounds (e.g. 2.531(3) Å in the bis-PMePh₂ complex [14] and 2.482(2) Å in the bis-PMe₃ complex [18]); therefore it is logical to suppose that the Mo–PPh₃ bond is more susceptible to dissociation. The X-ray structure of CpMoCl₂(PEt₃)₂ has not been previously reported; therefore we proceeded to obtain one. Two polymorphs have been obtained under slightly different recrystallization conditions, these exhibiting the same geometry and metric parameters within experimental error (see Table 4).

An ORTEP view of the CpMoCl₂(PEt₃)₂ molecule is shown in Fig. 2. The geometry and all the other main features of the structure parallel those previously reported and discussed for similar CpMoCl₂L₂ molecules (L = PMe₃ [18],

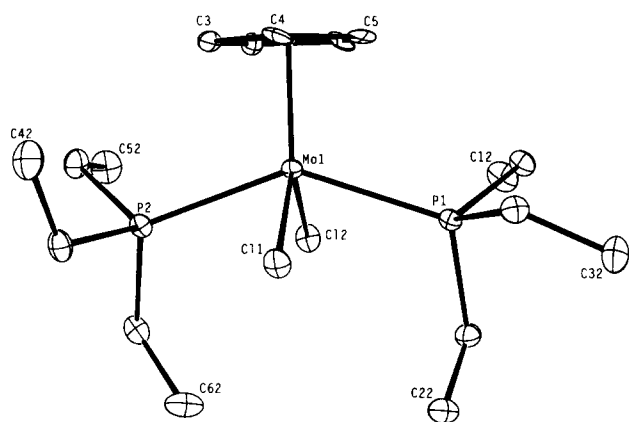
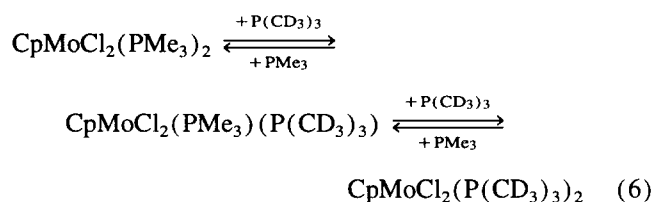


Fig. 2. An ORTEP view of the $\text{CpMoCl}_2(\text{PEt}_3)_2$ molecule with ellipsoids shown at the 30% probability level. Only the major orientation of the Cp ring is shown and hydrogen atoms have been omitted for clarity.

PMePh_2 and PPh_3 [14], or $\text{L}_2 = \text{dppe}$ [13]) and for $\text{Cp}^*\text{MoCl}_2(\text{PMe}_3)_2$ [15]. For the purpose of the present study, the only interesting parameter is the Mo–P distance, which is on average $2.528(1) \text{ \AA}$, i.e. slightly shorter than the same distance in the PPh_3 analog, and much longer than that in the PMe_3 analog. This trend parallels the steric bulk as measured by the phosphine cone angle (PPh_3 , 145° ; PEt_3 , 132° ; PMe_3 , 118°) [17].

A dissociative exchange and a correlation between the rate of phosphine dissociation and the Mo–P distance lead to the expectation of a very slow phosphine exchange for compound $\text{CpMoCl}_2(\text{PMe}_3)_2$. Since this is the most stable phosphine system, only the self-exchange could be conveniently measured. For this purpose, reactions of $\text{CpMoCl}_2(\text{PMe}_3)_2$ with various excess amounts of $\text{PMe}_3\text{-}d^9$ were measured, using ^1H NMR spectroscopy at 27°C to follow the growth of the free PMe_3 resonance. This is a degenerate equilibrium system involving two separate steps:



A detailed kinetic analysis by fitting the observed data to an integrated rate law would be quite complex. We elected to use the more straightforward analysis of the initial rates, which were measured up to less than 25% exchange, under pseudo-first-order conditions and as a function of excess $\text{PMe}_3\text{-}d^9$ (results in Table 1).

Indeed, the exchange is extremely slow compared to the other systems studied, several hours being necessary at room temperature to achieve even a small percent of the exchange. The values of k_{obs} as a function of initial $[\text{PMe}_3\text{-}d^9]$ are plotted in Fig. 3. The initial rate of the reaction depends on the $\text{PMe}_3\text{-}d^9$ concentration, but the straight line best fitting the experimental points does not intercept the origin. Therefore, a two-term rate law:

$$k_{\text{obs}} = k_1 + k_2[\text{P}(\text{CD}_3)_3] \quad (7)$$

is indicated, with a first-order (dissociative) term k_1 corresponding to path (a) of Scheme 1, and a second-order (associative) term k_2 , corresponding to path (b). The value of k_1 obtained from this graph is reported in Table 6.

It is clear, therefore, that the smaller and better binding PMe_3 ligand slows down the dissociative process to a point where the alternative associative path, which proceeds either through a sterically crowded 19-electron intermediate or, more likely, through a ring-slipped (also quite crowded) 17-electron intermediate, becomes competitive. It should be remarked that bulkier and less basic phosphines are expected to react more slowly than PMe_3 in an associative fashion. This gives further credit to the previous assertion that the more rapid phosphine exchange reactions in Eqs. (1)–(5) are dissociative in nature.

Further and conclusive proof that the most important path for the phosphine exchange is dissociative is provided by a comparison between the PMe_3 self-exchange process just described and the corresponding process of the related Cp^* system:

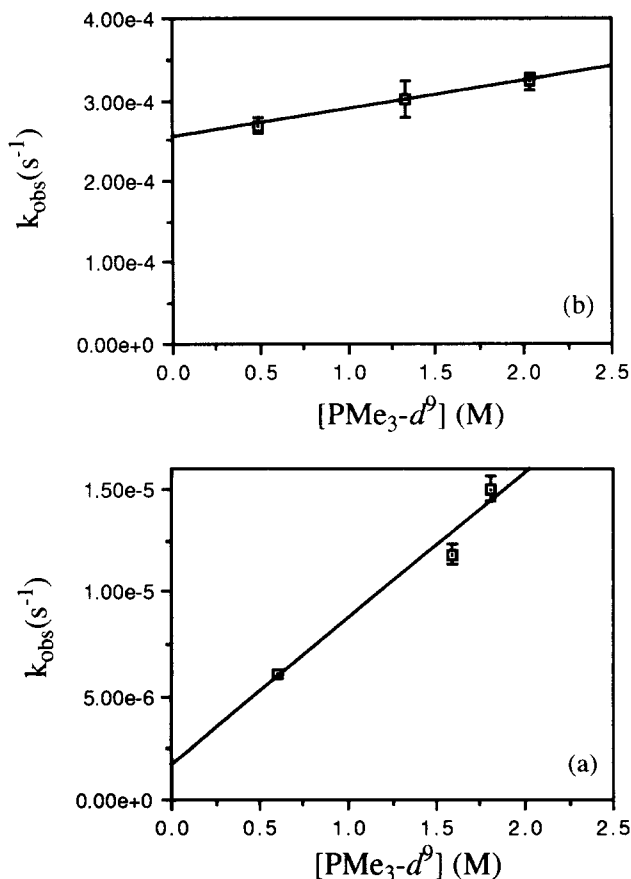
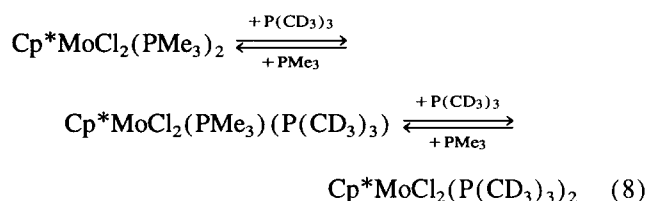


Fig. 3. Values of k_{obs} from initial rates for the $\text{CpMoCl}_2(\text{PMe}_3)_2/\text{PMe}_3\text{-}d^9$ exchange (a) and for the $\text{Cp}^*\text{MoCl}_2(\text{PMe}_3)_2/\text{PMe}_3\text{-}d^9$ exchange (b). Solvent C_6D_6 ; $T = 27^\circ\text{C}$.



This process was analyzed exactly as described above for the Cp counterpart, e.g. by determining the initial rates of exchange as a function of excess amount of PMe_3 - d^9 under pseudo-first-order conditions with ^1H NMR monitoring. The measured k_{obs} values are collected in Table 1 and shown in Fig. 3. The first observation to be made is that this reaction is over one order of magnitude faster than for the corresponding Cp system. If the phosphine exchange were to occur prevalently via an associative mechanism, the exchange should have been *slower* on the electron-rich and more crowded Cp^* complex. Secondly, there is little effect of $[\text{PMe}_3$ - d^9] on the initial rates. The slope of the linear fit of the data (k_2 in Eq. (7)) is small compared to the error in this parameter and, although a parallel second-order pathway may in fact be operative also for this exchange, we cannot exclude that the small deviation of the straight line from horizontal is caused by subtle experimental factors such as the variation of the solvent nature due to the use of large excess amounts of PMe_3 - d^9 . The value of the first-order rate constant, obtained from the intercept of Fig. 3, is reported in Table 6. This self- PMe_3 exchange, therefore, proceeds essentially by a pure dissociative pathway for the Cp^* system. The rate increase for PMe_3 dissociation on going from Cp to Cp^* (over two orders of magnitude) can be explained by both ground state and transition state effects: the Cp^* starting compound is sterically more congested, as shown by the *longer* Mo–P distance in this system (2.509(1) Å) [15], and the 15-electron mono-phosphine intermediate can better be stabilized by the more electron-releasing Cp^* group. We now defer further consideration of the phosphine exchange mechanism to Section 4 and turn our attention to a couple of related observations.

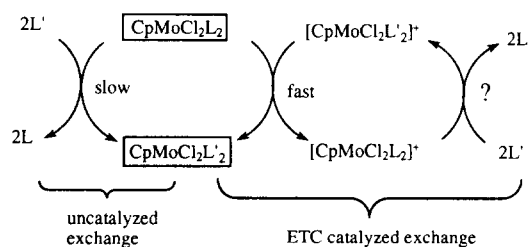
3.2. Exchange of chloride by phosphine

During the very slow PMe_3 self-exchange study on $\text{CpMoCl}_2(\text{PMe}_3)_2$, monitoring of the reaction was continued for several days aiming at determining the final equilibrium position of Eq. (6). However, this was prevented by the precipitation, after a few days at room temperature, of an orange microcrystalline material. This solid was recovered from the NMR tube and investigated spectroscopically. Its EPR spectrum matches that previously reported for compound $[\text{CpMoCl}(\text{PMe}_3)_3]^+\text{PF}_6^-$ [19], and shown in Fig. 1 of Ref. 19. On this basis, we propose that this orange solid is $[\text{CpMoCl}(\text{PMe}_3)_3]^+\text{Cl}^-$, obtained by slow exchange of a Cl^- ligand by PMe_3 . The low polarity of the solvent (C_6D_6) is responsible for precipitation and therefore accumulation of this product. When the compound is dissolved and left in

CH_2Cl_2 without any excess PMe_3 , it slowly (several hours at r.t.) converts back to $\text{CpMoCl}_2(\text{PMe}_3)_2$ with release of PMe_3 . It is worth noting that a similar salt, $[\text{CpMoCl}(\text{PMe}_3)_3]^+(\text{ZnCl}_3^-)$, formed rapidly when CpMoCl_2 and excess PMe_3 were allowed to react in the presence of the Lewis acidic ZnCl_2 , and that this salt also slowly converted to $\text{CpMoCl}_2(\text{PMe}_3)_2$ in CH_2Cl_2 when treated with an excess amount of a soluble chloride source [19].

3.3. Effect of oxidation on phosphine exchange

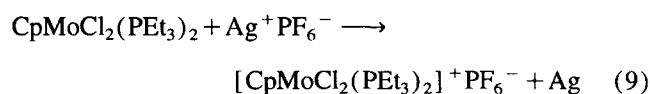
Since it had been previously established that the halide exchange reaction on $\text{CpMoX}_2(\text{PMe}_3)_2$ is catalyzed by an electron transfer chain (ETC) [20] process via oxidation to cationic Mo(IV) compounds [21], the possibility that a similar ETC process might take place for the phosphine exchange (Scheme 2) had to be considered and addressed. In other words, it is conceivable that the very fast phosphine exchange processes described by Eqs. (3)–(5) are so fast because they are in fact proceeding through a catalyzed mechanism, perhaps because of adventitious oxidation as is the case for the halide exchange [21], and that the uncatalyzed exchange would in fact be slow. The electron transfer step of such an ETC mechanism must be very fast, since all $\text{CpMoCl}_2\text{L}_2$ systems investigated by us undergo chemically reversible oxidative electrochemistry, and two pairs of $[(\text{Ring})\text{MoCl}_2\text{L}_2]^{n+}$ ($n=0, 1$) complexes (i.e. Ring = Cp, L = PMe_3 [18], and Ring = Cp^* , L = PMe_2Ph [22]) have been crystallographically characterized as isostructural pairs with only very minor readjustments of bond distances and angles. There are a few remaining questions to be addressed. (a) Is the electron transfer end- or ex-ergonic? (An endergonic electron transfer step would result in an inefficient ETC catalyst [20].) (b) How fast is ligand exchange in the 16-electron manifold? Obviously, oxidation at the metal would be expected to speed up an associative reaction and to slow down a dissociative one. In order to answer these questions, we investigated the $\text{CpMoCl}_2(\text{PET}_3)_2/\text{dppe}$ exchange.



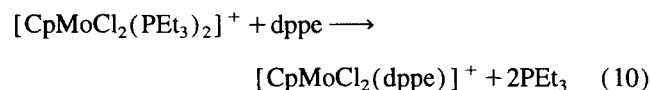
Scheme 2.

It has been determined that $[\text{CpMoCl}_2(\text{dppe})]^+$ is a stronger oxidant than $[\text{CpMoCl}_2(\text{PET}_3)_2]^+$ ($E_{1/2} = -0.33$ and -0.61 V versus fc/fc^+ , respectively). Therefore, the electron transfer is thermodynamically favorable, a necessary condition for an efficient ETC catalysis for the $\text{CpMoCl}_2(\text{PET}_3)_2/\text{dppe}$ exchange. The rate of exchange in the 16-electron cationic complexes was probed initially by cyclic voltammetry on a solution containing $\text{CpMoCl}_2(\text{PET}_3)_2$ and

a large excess of dppe. The triethylphosphine complex gave a reversible oxidation wave and there was no significant growth of the wave due to the $[\text{CpMoCl}_2(\text{dppe})]/[\text{CpMoCl}_2(\text{dppe})]^+$ system following production of $[\text{CpMoCl}_2(\text{PEt}_3)_2]^+$ on the electrode. Continued monitoring by CV indicated that the growth of the oxidation wave due to the dppe complex at -0.33 V qualitatively corresponded to the (uncatalyzed) rate of its formation, as previously determined by EPR (see above). This experiment demonstrates that the PEt_3/dppe exchange at the level of the Mo(IV) cationic complex is slow with respect to the time scale of a CV run (about 1 min). In order to have more direct information about the $[\text{CpMoCl}_2(\text{PEt}_3)_2]^+/\text{dppe}$ exchange, we have generated the Mo(IV) cation stoichiometrically by oxidation of the corresponding Mo(III) parent compound as shown in



and subsequently monitored the phosphine exchange of



by ^1H and ^{31}P NMR spectroscopy.

We limited the characterization of the previously unreported $[\text{CpMoCl}_2(\text{PEt}_3)_2]^+ \text{PF}_6^-$ compound by ^1H NMR in comparison with the spectrum of the related $[\text{CpMoCl}_2(\text{PMe}_3)_2]^+$ that was generated by the same method [21]. The resonances are paramagnetically shifted, the chemical shifts being linearly dependent on the inverse temperature (see Fig. 4), as expected for a Curie paramagnet. Compound $[\text{CpMoCl}_2(\text{PMe}_3)_2]^+$ was also shown to be paramagnetic ($S = 1$ ground state) [18]. At room temperature, the Cp protons resonate at δ 180.0 (cf. 179.5 for the PMe_3 analog), and the phosphine α -protons (methylene) are at δ -5.26 (cf. -6.6 for the methyl protons in the PMe_3 analog). The methyl protons in the PEt_3 compound (in β position with respect to P) are found at δ 7.93. Upon introduction of excess dppe, no significant change is observed in the ^1H NMR spectrum at room temperature over 6 h (under the same conditions, the exchange on the Mo(III) parent complex would be essentially complete). Correspondingly, the ^{31}P NMR shows no evidence for the formation of free PEt_3 . It is clear, therefore, that the phosphine exchange is not faster but rather *slower* on Mo(IV) with respect to Mo(III) . This is consistent with a dissociative phosphine substitution on Mo(III) and with the absence of ETC catalysis in this system.

The reason for the very different behavior between phosphine exchange and halide exchange on the same Mo(III) system (the latter being a slow *associative* exchange and being catalyzed by oxidative ETC) [16,21] must have its origin in the size and charge of the ligand being exchanged. For the halide exchange, while a dissociative path on the 17-electron system is disfavored by the separation of charge, oxidation to the Mo(IV) 16-electron *cationic* species pro-

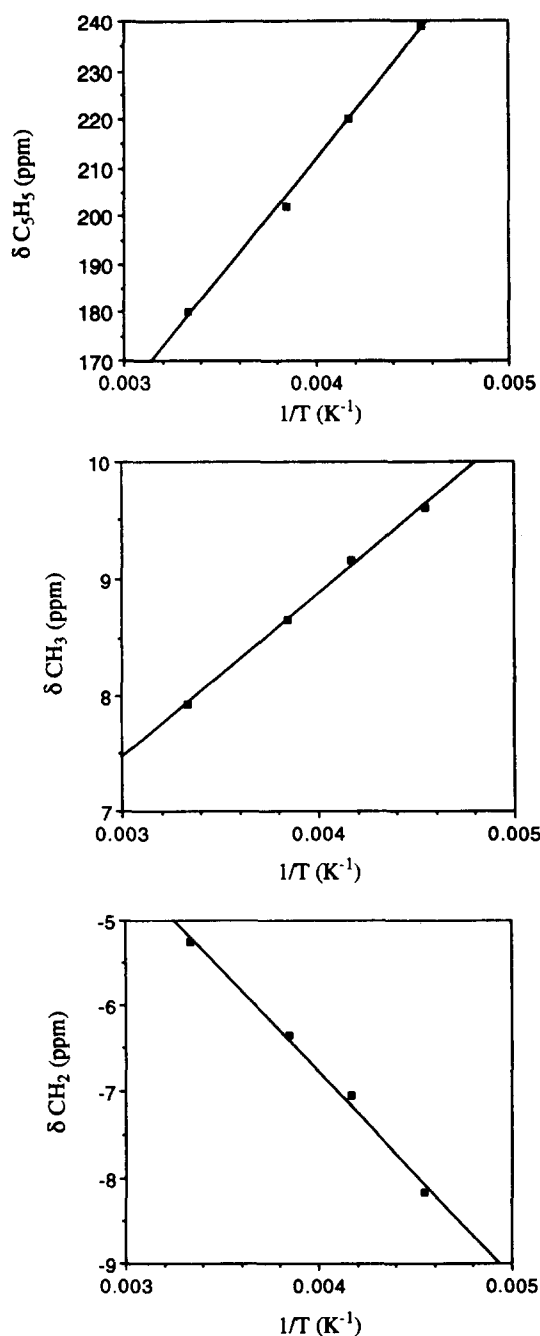


Fig. 4. Variable temperature chemical shifts for the resonances of compound $[\text{CpMoCl}_2(\text{PEt}_3)_2]^+$: (a) Cp resonance; (b) PEt_3 methyl resonance; (c) PEt_3 methylene resonance. Solvent CD_2Cl_2 .

vides a formidable acceleration for the addition of the negatively charged (and relatively small) halide ion.

4. Discussion

The results shown above for a series of phosphine exchange processes on 17-electron (Ring) MoCl_2L_2 systems (Ring = Cp, Cp^* ; L = tertiary phosphine) show that the most important exchange mechanism is dissociative and therefore presumably involves unsaturated 15-electron intermediates.

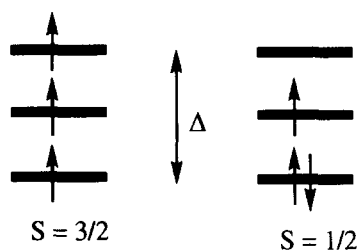


Fig. 6. Generic energy diagram for the metal-based molecular orbitals in a 15-electron CpMoX_2L -type system.

having a formal 15-electron count), e.g. $\text{MoCl}_3(\text{PR}_3)_3$ ($\text{PR}_3 = \text{PMe}_2\text{Ph}, \text{PEt}_2\text{Ph}$, etc.), have three unpaired electrons ($S = 3/2$) as expected from the pseudo- t_{2g}^3 electronic configuration [30]. Stable cyclopentadienylchromium(III) compounds of general formula CpCrX_2L are pseudo-octahedral systems when considering that the Cp ligand formally occupies three coordination positions and are isostructural and isoelectronic with our proposed dissociative CpMo(III) intermediates; these also have an $S = 3/2$ ground state [31], although their low symmetry removes the degeneracy of the pseudo- t_{2g} levels. Our attempts to isolate models for the dissociative CpMo(III) intermediate have so far failed [22]¹. Assuming, however, by extension of the above-mentioned chromium work, that 15-electron Mo(III) CpMoX_2L -type complexes would also have an $S = 3/2$ ground state, we then expect a contribution to electronic stabilization due to the spin state change on going from the 17-electron starting material ($S = 1/2$) [18] to the intermediate. This stabilization effect should be greater the more stabilized the $S = 3/2$ state with respect to the $S = 1/2$ state, this in turn depending on the relative magnitude of the orbital splitting Δ (Fig. 6) and the pairing energy P , but how large this effect is in this particular case (or even whether it exists) remains currently unknown. We believe that this effect of a spin state change can play an important role in organometallic reactivity, especially for systems where the pairing energy is expected to be high. We are currently pursuing experimental and theoretical studies on models of the dissociative 15-electron intermediate with the goal of determining its ground state magnetic properties and the magnitude of the triplet–singlet energy gap.

5. Conclusions

We have demonstrated here that the dissociative phosphine substitution reaction on the cyclopentadienyl Mo(III) system $\text{CpMoCl}_2(\text{PR}_3)_2$ is inherently faster than the associative one and have proposed ligand π -donation and spin state change as responsible for the stabilization of the unsaturated 15-electron intermediate. In this respect, this chemistry may be seen as a bridge between classical low-oxidation state organometallic chemistry, where the energetics is dominated by

¹ Note added in proof: we now have preliminary results indicating that complex $[\text{Cp}^*\text{MoCl}(\text{dppe})]^+$ may be sufficiently stable to be isolated.

bond enthalpies and the 18-electron rule, and coordination chemistry, where the geometry and the spin state are of primary importance. In fact, the proposed intermediate of the reactions shown here, the 15-electron $\text{CpMoCl}_2(\text{PR}_3)_2$ system, is isolobal with stable Mo(III) coordination compounds.

6. Supplementary material

A detailed description of the data collection and the structure solution and refinement, full tables of bond distances and angles, anisotropic displacement parameters, hydrogen atom coordinates, and calculated and observed structure factors for $\text{CpMoCl}_2(\text{PEt}_3)_2$ (36 pages) are available from the authors on request. The crystallographic tables have also been deposited with the Cambridge Crystallographic Data Centre.

Acknowledgements

This work was supported by awards to R.P. from the NSF (PYI 1990-95, CHE-9058375) and the Alfred P. Sloan Foundation (Research Fellowship, 1992–94). We also thank the NSF for an instrumentation grant for the upgrade of the EPR spectrometer (CHE-9225064). R.P. wishes to thank Professor Fred Basolo for helpful comments on this work and also for much appreciated encouragement and friendship.

References

- [1] F. Basolo, *Polyhedron*, 9 (1990) 1503–1535.
- [2] F. Basolo, *Coord. Chem. Rev.*, 100 (1990) 47–66.
- [3] J.D. Atwood, *Inorganic and Organometallic Reaction Mechanisms*, Brooks/Cole, Monterey, CA, 1985.
- [4] R.H. Crabtree, *The Organometallic Chemistry of the Transition Metals*, Wiley, New York, 1994.
- [5] C.A. Tolman, *Chem. Soc. Rev.*, 1 (1972) 337.
- [6] W.C. Trogler (ed.), *Organometallic Radical Processes*, Elsevier, Amsterdam, 1990.
- [7] A. Fox, J. Malito and A. Pož, *J. Chem. Soc., Chem. Commun.*, (1981) 1952–1953.
- [8] T.R. Herrington and T.L. Brown, *J. Am. Chem. Soc.*, 107 (1985) 5700–5703.
- [9] Q.-Z. Shi, T.G. Richmond, W.C. Trogler and F. Basolo, *J. Am. Chem. Soc.*, 106 (1984) 71–80.
- [10] A.E. Stiegman and D.R. Tyler, *Comments Inorg. Chem.*, 5 (1986) 215.
- [11] R.M. Kowaleski, F. Basolo, W.C. Trogler, R.W. Gedridge, T.D. Newbound and R.D. Ernst, *J. Am. Chem. Soc.*, 109 (1987) 4860–4869.
- [12] R.G. Linck, B.E. Owens, R. Poli and A.L. Rheingold, *Gazz. Chim. Ital.*, 121 (1991) 163–168.
- [13] S.T. Krueger, B.E. Owens and R. Poli, *Inorg. Chem.*, 29 (1990) 2001–2006.
- [14] R. Poli, B.E. Owens, S.T. Krueger and A.L. Rheingold, *Polyhedron*, 11 (1992) 2301–2312.
- [15] R.T. Baker, J.C. Calabrese, R.L. Harlow and I.D. Williams, *Organometallics*, 12 (1993) 830.

- [16] R. Poli, B.E. Owens and R.G. Linck, *Inorg. Chem.*, *31* (1992) 662–667.
- [17] C.A. Tolman, *Chem. Rev.*, *77* (1977) 313–348.
- [18] S.T. Krueger, R. Poli, A.L. Rheingold and D.L. Staley, *Inorg. Chem.*, *28* (1989) 4599–4607.
- [19] F. Abugideiri, M.A. Kelland, R. Poli and A.L. Rheingold, *Organometallics*, *11* (1992) 1303–1311.
- [20] D. Astruc, *Angew. Chem., Int. Ed. Engl.*, *27* (1988) 643–660.
- [21] R. Poli, B.E. Owens and R.G. Linck, *J. Am. Chem. Soc.*, *114* (1992) 1302–1307.
- [22] F. Abugideiri, D.W. Keogh, H.-B. Kraatz, R. Poli and W. Pearson, *J. Organomet. Chem.*, *488* (1995) 29–38.
- [23] N.C. Hallinan, G. Morelli and F. Basolo, *J. Am. Chem. Soc.*, *110* (1988) 6585–6586.
- [24] J.K. Shen, J.W. Freeman, N.C. Hallinan, A.L. Rheingold, A.M. Arif, R.D. Ernst and F. Basolo, *Organometallics*, *11* (1992) 3215–3224.
- [25] T.D. Newbound, A.L. Rheingold and R.D. Ernst, *Organometallics*, *11* (1992) 1693–1700.
- [26] J.W. Freeman, N.C. Hallinan, A.M. Arif, R.W. Gedridge, R.D. Ernst and F. Basolo, *J. Am. Chem. Soc.*, *113* (1991) 6509–6520.
- [27] R. Poli, *J. Coord. Chem.*, *B29* (1993) 121–173.
- [28] R.G. Pearson and F. Basolo, *J. Am. Chem. Soc.*, *78* (1956) 4878–4883.
- [29] K.G. Caulton, *New J. Chem.*, *18* (1994) 25–41.
- [30] M.W. Anker, J. Chatt, G.J. Leigh and A.G. Wedd, *J. Chem. Soc., Dalton Trans.*, (1975) 2639–2645.
- [31] E.O. Fischer, K. Ulm and P. Kuzel, *Z. Anorg. Allg. Chem.*, *319* (1963) 253–265.